Fuel 94 (2012) 184–190

Contents lists available at SciVerse ScienceDirect

Fuel

journal homepage: www.elsevier.com/locate/fuel

Increased particle emissions from early fuel injection timing Diesel low temperature combustion

Jesús Benajes, José M. García-Oliver, Ricardo Novella, Christopher Kolodziej *

CMT – Motores Térmicos, Universidad Politécnica de Valencia, Camino Vera s/n, 46022 Valencia, Spain

ARTICLE INFO

Article history:
Received 15 March 2011
Received in revised form 1 September 2011
Accepted 5 September 2011
Available online 28 September 2011

Keywords:
Diesel engine
Particle
Emissions
Premixed
Low temperature combustion

ABSTRACT

A clean premixed Diesel combustion strategy, called low temperature combustion (LTC), was able to achieve very low nitrogen oxide emissions (<35 ppm) through use of exhaust gas recirculation (12.1% inlet oxygen), and reduced particulate matter (PM) emissions (<0.05 FSN) through advanced fuel injection timing (−24°aTDC). When varying the injection timing by relatively small increments, large changes in PM mass and number emissions were measured within the premixed LTC regime. A discrepancy is investigated between expected reductions in PM emissions by simple fuel–air premixing and combustion temperature metrics, and actual PM emissions measurements when advancing the fuel injection timing earlier than −24°aTDC. For these earlier injection timings, particle numbers were seen to increase in two distinct particle size modes, whereas only one particle size mode existed at the minimum PM emissions −24°aTDC injection timing. Additional parameters from a 1D free fuel spray model were used to suggest new information that could explain the cause of these unexpected increases in PM. Using 0D and 1D calculations, the engine-out particle size and number emissions are analyzed to better understand their sensitivity to changes in the fuel injection timing within the early injection timing LTC regime.

1. Introduction

Diesel engines offer an inherent advantage of reduced fuel consumption and CO_2 emissions over other types of internal combustion engines due to their higher thermal efficiency. For this reason the Diesel engine is a common powerplant option for transportation, especially in medium and heavy duty vehicles. The drawback of conventional Diesel engines is their traditionally higher emissions levels of particulate matter (PM) and oxides of nitrogen (NO_x). Many researchers [1–4] have shown evidence of a correlation of ambient particle levels with hospital admissions and mortality rates (strongest correlations with respiratory and cardiovascular system ailments). Other studies [5–11] have suggested the importance of the ultrafine portion (smaller than 100 nm) of all ambient particles on health effects. Diesel engines have been shown to emit a great deal of their particles (especially in particle number) in the ultrafine size range [12,13]. Therefore understanding the particle emissions characteristics from conventional and modern Diesel engines is important to better understanding their effects on the environment and human health.

New emissions regulations are obliging engine manufacturers to reduce these emissions far below previous levels. In-cylinder formation of Diesel soot aggregate particles occur in regions of high local richness and temperature [14,15]. Enhancing the fuel and air mixing process in-cylinder before the start of combustion (SOC) and reducing the adiabatic flame temperature by the use of exhaust gas recirculation (EGR) in the Low Temperature Combustion (LTC) regime with modern Diesel engines has helped to decrease engine-out particulate matter (PM) mass emissions [16–20].

Although these LTC combustion concepts have greatly reduced engine-out PM mass emissions in comparison with conventional Diesel combustion, more comprehensive particle emissions measurements have shown a simultaneous decrease in the particle sizes, increase in particle organic fraction (volatility), and (depending on the LTC engine operating condition) a possible increase in particle numbers [21–26]. Recent publications [20,27–29] have shown that there can exist an early and a late fuel injection timing within the Diesel LTC regime, for a given engine load and speed, where engine-out PM emissions are possible at (or below) the minimum detection limit of a common opacity-based PM mass concentration measurement instrument. It was described that although the PM mass emissions had been greatly reduced relative to conventional Diesel combustion, important changes still occurred in particle size and number emissions within the LTC regime (especially for particles smaller than 50 nm) [28,29]. In [28], advancement of the fuel injection timing from the timing of maximum PM (−9°aTDC) emissions led to elongation of the ignition delay (time from start of injection to start of combustion) and decreases in emissions of particulate mass and number concentrations. Thermodynamic calculations indicated that further increases in the ignition delay were possible with continued

* Corresponding author. Tel.: +34 963877650; fax: +34 963877659.
E-mail addresses: chko@mot.upv.es, ckolodziej@hotmail.com (C. Kolodziej).

0016-2361/$ - see front matter © 2011 Elsevier Ltd. All rights reserved.
doi:10.1016/j.fuel.2011.09.014

Nomenclature

%_vol	Percent by volume	g/kg$_{fuel}$	Mass pollutant per mass fuel injected
°aTDC	Degrees after top dead center	HC	Hydrocarbon
0D	Zero dimensional	IMEP	Indicated mean effective pressure
1D	One dimensional	Local Φ_{SOC}	Local equivalence ratio at SOC
CAD	Crank angle degree	LTC	Low temperature combustion
CO	Carbon monoxide	m/m	Fraction mass per mass
CO_2	Carbon dioxide	NO_x	Oxides of nitrogen
CPC	Condens. particle counter	PAH	Polycyclic aromatic hydrocarbon
DMA	Differential mobility analyzer	PM	Particulate matter
$dN/d\log D_p$	Normalized and number-weighted particle concen.	RPM	Revolutions per minute
EGR	Exhaust gas recirculation	SMPS	Scanning mobility particle sizer
Flame T_{ad}85	Adiabatic flame temp. after 85% fuel mass burned	SOC	Start of combustion
FSN	Filter smoke number		

advancement of the injection timing beyond the point where PM emissions were already below the opacity-based instrument's minimum detection limit, thus predicting a further reduction in particulate mass and number emissions. But emissions measurements showed otherwise, that both PM mass and number emissions increased with further injection timing advances beyond the injection timing of the opacity-based instrument's minimum detection limit (−24°aTDC). The particle size distribution results revealed that there were increases in two distinct modes of particles, at 20 nm and 100 nm when the injection timing was advanced. Using a 1D free spray analysis model [30,31], this work investigates if fuel spray-piston surface interactions caused PM mass and number emissions increases for further advanced injection timings within the Diesel LTC regime, though ignition delay and adiabatic flame temperature towards the end of combustion both increased (reasons for decreases in engine-out PM emissions) with further advancements of fuel injection timing.

2. Materials and methods

2.1. Engine

The characteristics of the Diesel research engine used in this study are described in Table 1. The engine hardware was selected so that it could effectively operate in either the conventional Diesel mixing-controlled, or Diesel premixed LTC operating regime throughout the entire engine load and speed map.

Table 2 illustrates the engine operating conditions selected for this study. The range of injection timings selected for this study, −24 to −33°aTDC, was selected to study the sensitivity of increased PM mass and number emissions with injection timing advancements earlier than the early minimum PM injection timing (−24°aTDC). The earliest injection timing in the study was limited to −33°aTDC to maintain in-cylinder pressure rise rates less than 22 bar/CAD. An intake oxygen concentration of 12.1% proved to be low enough to reduce the maximum adiabatic flame temperature below 2200 K, and the NO_x emissions below 35 ppm (1.09 g/kg$_{fuel}$). The intake temperature, intake pressure, and EGR rate were selected to achieve a LTC engine operating condition while being consistent with realistic pre-production heavy duty Diesel engine capabilities.

Table 1
Engine characteristics.

Engine type	Single cylinder, direct-injection, four-stroke
Bore × stroke (mm)	123 × 152
Displacement (l)	1.806
Compression ratio (–)	14.4:1
Injector nozzle	Mini-Sac, 7 × 0.190 mm
Injector included Angle (°)	120

Table 2
LTC engine operating conditions.

Speed (RPM)	1200
IMEP (bar)	≈7
Fuel injected (mg/cycle)	70
Start of Injection (°aTDC)	−24 to −33
Injection pressure (bar)	1450
EGR (%_vol)	50
Intake oxygen (%_vol)	12.1
Equivalence ratio (–)	0.83
Intake temperature (°C)	45
Intake pressure (bar)	1.35
Exhaust temperature (°C)	366
Exhaust pressure (bar)	1.45

A commercially available European Diesel fuel was used in this study with a cetane number of 53.5, sulful content of 8.9 ppm, PAH content of 1.3% (m/m), and a T95 of 356 °C. These specific fuel properties were analyzed due to their known influence on combustion generated nanoparticle emissions [32–36].

2.2. Emissions instruments

A Horiba MEXA 7100 was used to measure the exhaust gaseous components of carbon dioxide (CO_2), carbon monoxide (CO), hydrocarbons (HC), and oxides of nitrogen (NO_x). An AVL Smokemeter 415 (opacity-based measurement) was used to measure the exhaust PM mass concentration. In order to make measurements of the particle size distribution with a TSI Scanning Mobility Particle Sizer (SMPS), a dual-stage partial exhaust dilution was performed using a Dekati FPS-4000.

The exhaust sample temperature was measured to be 295 °C in the engine exhaust system at the point where the exhaust sample was extracted by the dilution system. The dilution system inlet sample probe temperature was regulated as close as possible (but not exceeding) the exhaust sample temperature, at 290 °C. The primary dilution heater setpoint temperature was set to the maximum recommended by the diluter manufacturer, 300 °C. The actual temperature of the primary dilution air once it entered the diluter body, as measured by an internal thermocouple just before the point of mixing with the exhaust sample, was 182 °C due to heat losses during flow to the diluter body. Although the primary dilution was performed with 5.9 lpm of heated dilution air, the 162 lpm of secondary dilution air was used at ambient temperature. The secondary dilution air flow was maximized for this diluter and the primary dilution air flow was adjusted to achieve the overall 40:1 total dilution ratio.

The TSI SMPS 3936 consisted of the TSI 3080L electrostatic classifier with a long Differential Mobility Analyzer (DMA) and a TSI 3010 Condensation Particle Counter (CPC). Fig. 1 shows a schematic of the SMPS 3936 component setup. Particle concentration units of the size distribution are displayed in $dN/d\log D_p$ (particle number per cubic centimeter), meaning that the particle number concentration has been weighted by particle number (the instrument's base unit) and normalized to one decade of particle size so that particle size distributions from various instruments can be compared independent of their channel resolution [37].

2.3. 1D fuel spray model

Since the end of fuel injection occurred prior to the start of combustion in all injection timings studied, a 1D mixing-controlled inert Diesel spray model could be applied to predict such parameters as the maximum local fuel–air equivalence ratio at the start of combustion and the maximum free spray liquid length during the injection event [30,31].

The model solves momentum and fuel mass conservation equations for the spray. To simplify the spatial description of both properties, self-similar Gaussian profiles are assumed, which makes it possible to transform a 2D problem (if symmetry is assumed) into a 1D one. The spray is discretized along its axis in Δx size cells that occupy the whole flow cross-section, and for each cell only on-axis properties are solved. In a second step, radial distribution of properties can be obtained by corresponding self-similar profiles.

To complete the spray description, both conservation equations are coupled to state relationships, which form some kind of equation of state for the fuel–air mixture, where any property is calculated from the ideal mixing of pure air and pure fuel. In that way, any relevant spray property (composition, temperature, density) can be expressed as a function of fuel mass fraction. The approach is valid as long as the assumptions of 'mixing-controlled' processes can be used, which assumes processes within the spray to be mainly governed by air entrainment, and droplet transfer rates of mass and energy to be much faster.

The model has been developed to predict fuel spray behavior under transient conditions, such as a fuel spray into the combustion chamber of a Diesel engine during compression and expansion. One difference between the model and the engine combustion chamber is that the model has been designed to predict spray development in a large volume without wall effects, whereas the spray in the actual engine is affected by encountering combustion chamber surface areas (such as the piston bowl surface). These limitations of the model have been taken into account in this analysis and it should be noted that conclusions from the model are drawn on a qualitative basis, relative between each of the injection timings.

Since the 1D free spray model's inputs come from experimental test data, the results are believed to quite accurately represent the in-cylinder conditions occurring during the actual engine tests. One of these inputs to the model is a description of the instantaneous mass flow rate of the fuel spray actually being injected into the combustion chamber. Information regarding the start, end, and mass flow profile of the fuel injection event is derived from an experimental injection rate (fuel momentum) spray test, performed in the actual engine test cell, and using the same injection system hardware and software used during the actual engine tests. The principles of the injection spray test method have been based on those by Bosch [38]. The other input data set that the model requires is to generate the same environmental conditions in the model's large volume as in the engine. This data set includes details of the instantaneous in-cylinder pressure and density, mainly to reconstruct pure air properties and calculate the state relationships. This information is measured during the engine tests and prepared by a 0D thermodynamic code [39–41]. Based on these experimentally determined fuel spray mass flow rate and instantaneous in-cylinder conditions, the 1D free spray model can reliably calculate the in-cyinder fuel spray properties following each engine test.

3. Results and discussion

3.1. Combustion metrics

It has been established that in-cylinder particle formation occurs in the regions of high temperature and local richness of the combustion chamber [14,15]. Therefore the first parameters analyzed were those which can readily indicate the quality of in-cylinder PM formation and oxidation (Fig. 2). The first parameter used to predict the relative level of PM formation was the ignition delay (time from actual start of fuel injection to the start of the high temperature heat release), calculated from the previously mentioned fuel spray tests and a 0D thermodynamic analysis [39–41]. The

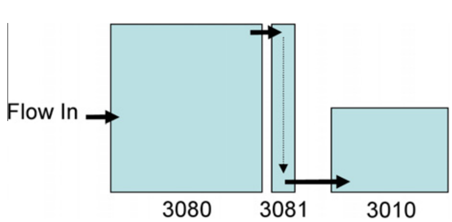

Fig. 1. Schematic of SMPS 3936 setup.

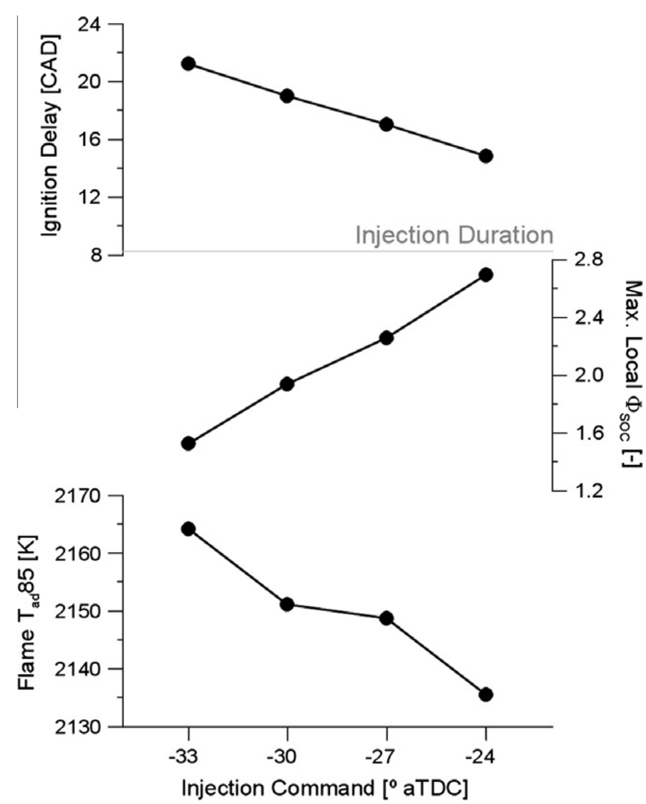

Fig. 2. Relative in-cylinder PM formation and oxidation metrics.

second parameter, which came from the 1D free fuel spray model, was the maximum local equivalence ratio of the injected fuel at the start of the combustion (start of high temperature heat release) within the open combustion chamber volume. Both of these first parameters suggest the level of fuel–air mixing before the start of combustion (SOC). Therefore the longer the ignition delay, and lower the maximum local fuel–air equivalence ratio at the SOC, the lower the PM formation should be (for similar temperature conditions). The third parameter, adiabatic flame temperature after 85% fuel mass burned (Flame T_{ad}85), considers the level of in-cylinder PM oxidation. The higher the Flame T_{ad}85, the more particles that are presumed to have been oxidized during the end of the combustion process.

From Fig. 2, it is possible to see that the ignition delay was longer than the injection duration in all injection timings studied. This means that the end of injection occurred before the start of combustion in all cases. Next seen was an increase in ignition delay and decrease in the local equivalence ratio at SOC with advances in injection timing earlier than −24°aTDC. Therefore, based on these two parameters, it can be presumed that in-cylinder PM formation should have decreased for earlier injection timings. Flame T_{ad}85 is shown to have increased with earlier injection timings. This suggests higher in-cylinder PM oxidation rates, and also supports decreased engine-out PM mass emissions with fuel injection timing advances earlier than −24°aTDC. Engine-out PM mass emissions are mostly based on the amount of particles formed minus the amount oxidized. Therefore these three parameters shown in Fig. 2 suggest further decreases in engine-out PM emissions with advances in injection timing because of both lower PM formation and higher PM oxidation.

3.2. General emissions

Fig. 3 shows the emissions measurements for injection timings advanced of −24°aTDC (the injection timing of minimum-PM early LTC). The values are represented in grams of the respective emission specie per kilograms of fuel injected. This emissions index has the advantage that it is not subject to the changes in engine power at the different injection timings. Further advances in injection timing showed increased PM mass, PM number, HC, and CO emissions. One can see a much higher increase in PM number emissions (>11-fold increase) from −30 to −33°aTDC than the relative increase in PM mass (>2-fold increase). Injection timing was not advanced past −33°aTDC due to elevated in-cylinder pressure rise rates (>22 bar/CAD).

The particle size distributions of the PM emissions for the injection timings tested are displayed in Fig. 4. A correlation can be seen between increased PM mass emissions and increases in number of particles larger than 50 nm in Figs. 3 and 4. The large increase in total particle number concentration from the −30 to −33°aTDC injection timing (half an order of magnitude) in Fig. 3 can be understood from not only the increase in particles larger than 50 nm, but also the even larger increase in particles smaller than 50 nm in the −33°aTDC injection timing. Montajir, et al. proposed a conceptual model of the characteristics of the particles in the Diesel PM particle size distribution [13]. They proposed that the particles of the accumulation mode (particles larger than approximately 50 nm) are primarily soot aggregates, conventionally produced in the locally fuel-rich/high temperature region inside a diffusive (mixing-controlled) Diesel flame. Although the PM formation and oxidation metrics from Fig. 2 predicted a decrease in engine-out PM and that all combustion cases investigated were only pre-mixed combustion (no diffusive Diesel flame), the actual emissions measurements from Figs. 3 and 4 showed increased PM emissions with advances in fuel injection timing. Possible explanations of this contradiction between combustion metrics and PM measurements will be discussed in the next section.

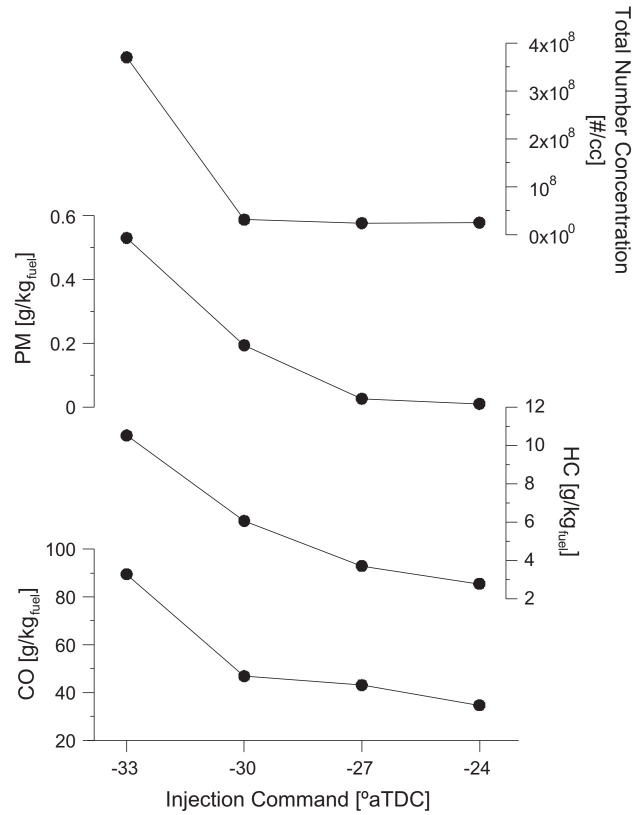

Fig. 3. Particulate matter, hydrocarbon, and carbon monoxide emissions.

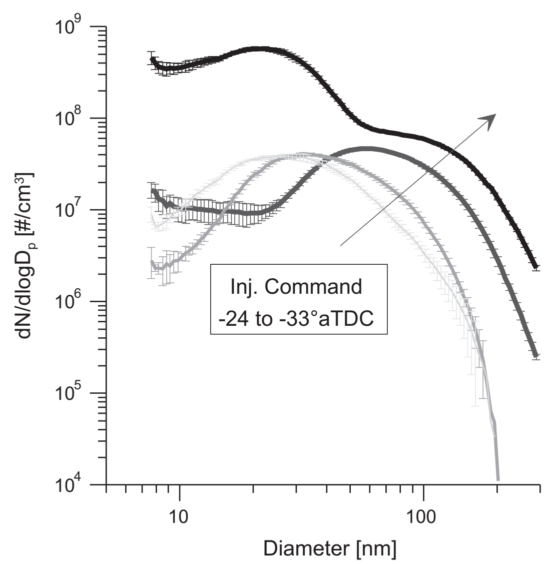

Fig. 4. Particle size distributions of tested injection timings.

3.3. Investigating the PM contradiction

Fig. 5 shows the trajectory of the fuel spray at the start of injection for each injection timing analyzed, projected onto the in-cylinder piston bowl surface. For advances in injection timing, the fuel spray trajectory crosses the piston bowl surface at a higher point (closer to the piston bowl lip).

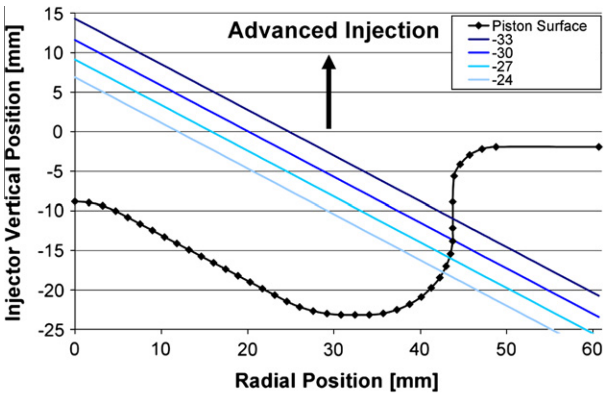

Fig. 5. In-cylinder fuel spray trajectory.

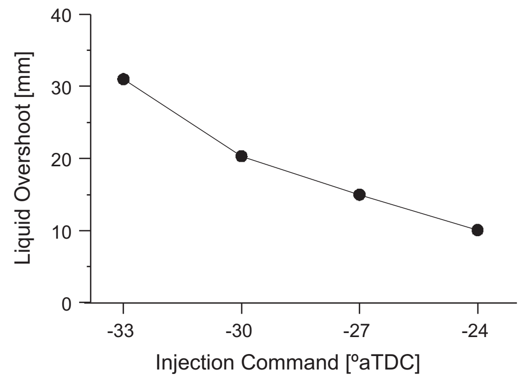

Fig. 6. Liquid spray overshoot behavior.

It is believed that advances in injection timing increased liquid fuel deposition on the piston bowl surface, caused by increased liquid fuel spray-combustion chamber surface interaction, thus increasing engine-out PM emissions. Increased in-cylinder PM formation from increased fuel deposition on the combustion chamber surface has been observed by in-cylinder optical measurements [42–45].

One way to investigate the relative level of fuel deposited on the piston bowl surface between each injection timing is to compare the maximum free spray liquid length (from the 1D free spray calculation) attained during the injection event for each injection timing to the distance from the injector nozzle to the piston bowl surface at that moment ("Distance to Piston" in Table 3). The 1D free spray model is capable of approximating the vapor spray length as well as the internal liquid spray length. Therefore analysis was performed using the maximum liquid spray length attained during the injection event and compared to the distance of the piston surface from the injector nozzle at that moment. The liquid overshoot shown in Table 3 approximates the length by which the maximum liquid length surpassed the piston bowl surface. This "overshoot" was calculated by subtracting the distance between the injector nozzle and the piston surface (at the instant of maximum liquid length) from the maximum liquid spray length predicted by the 1D free spray model. The liquid overshoot length can then be qualitatively representative of the liquid fuel deposited on the piston bowl surface.

In Fig. 6, increased liquid fuel spray overshoot past the piston bowl surface correlated with increased PM mass, PM number, HC, and CO emissions. Recalling that the requirements for PM formation are local fuel-richness and high temperatures (such as during the combustion process), this supports the idea that there was increased fuel deposition on the piston bowl surface for advances in injection timing earlier than −24°aTDC. Even at the −24°aTDC injection timing, there appeared to be some liquid fuel deposition on the piston bowl surface predicted. Although liquid fuel deposition on the piston bowl was predicted, the engine-out PM emissions were still very low. Therefore it is proposed that the combustion process was still able to sufficiently vaporize, mix, and oxidize the relatively smaller amount of fuel deposited on the piston bowl in the −24°aTDC injection timing condition. But further liquid fuel deposition on the piston bowl may have been too much to vaporize and mix before the SOC, thus contributing to the in-cylinder PM formation. This increased level of liquid fuel deposition resulted in increased PM mass, PM number, HC, and CO emissions.

Table 3
Maximum liquid spray length overshoot past piston.

Injection command (°aTDC)	−24	−27	−30	−33
Free spray max. liquid length (mm)	56.0	62.6	69.1	80.1
Distance to piston (mm)	45.9	47.6	48.8	49.1
Liquid overshoot (mm)	10.1	15.0	20.3	31.0

It is interesting to note that liquid overshoot increased by approximately 5 mm for every 3 CAD advance of the injection timing from −24 to −30°aTDC. But the increase in liquid overshoot from −30 to −33°aTDC was higher than the other injection timing intervals (approximately 8.7 mm). From Fig. 6 this higher increase in liquid overshoot from −30 to −33°aTDC compared well to the higher increase in total particle number concentration, PM mass concentration, HC, and CO than between the other injection timings.

Fig. 7 shows a comparison of liquid overshoot and PM emissions (by mass and number concentration). The axis ">50 nm Concentration" shows the sum of all channels for particles larger than 50 nm, normalized to $dN/d\log D_p$ particle concentration. The axis of "<50 nm Concentration" is likewise the sum of all $dN/d\log D_p$ normalized particle concentration channels smaller than 50 nm. As seen earlier in the particle size distributions, the total PM mass concentration correlates well with the number concentration of particles larger than 50 nm for advances in injection timing. This suggests, in agreement with Kittelson [12], that the particles in the accumulation mode (typically larger than 50 nm) have a larger influence on the total PM mass concentration than the particles smaller than 50 nm. Montajir, et al. have suggested that the accumulation mode of the size distribution is typically composed of aggregate particles which are typically formed in the high temperature and locally rich regions of a mixing-controlled, diffusive Diesel flame [13]. As displayed in Fig. 2, the end of injection occurred a few crank angle degrees (CAD) before the start of combustion in all injection timings analyzed in this study. This means that for these LTC engine operating conditions, there was not believed to have been an injected-fuel mixing-controlled diffusive Diesel flame to form soot aggregate particles. But the particle size distributions showed increased emissions of large accumulation mode particles (typically classified by Diesel PM researchers as soot aggregates) with advanced injection timings. Therefore it is proposed that although the fuel injection had finished, soot aggregate particles still indeed formed in a mixing-controlled difussion flame at these early injection timings. In these engine operating conditions, the aggregates are suggested to have come from a low mixing energy diffusion flame that existed on the piston bowl surface where liquid fuel had been deposited during the earliest injection timings. This diffusion flame on the piston bowl surface would be less-optimal than a conventional Diesel mixing-controlled diffusion flame because of the piston surface that would block air entrainment into

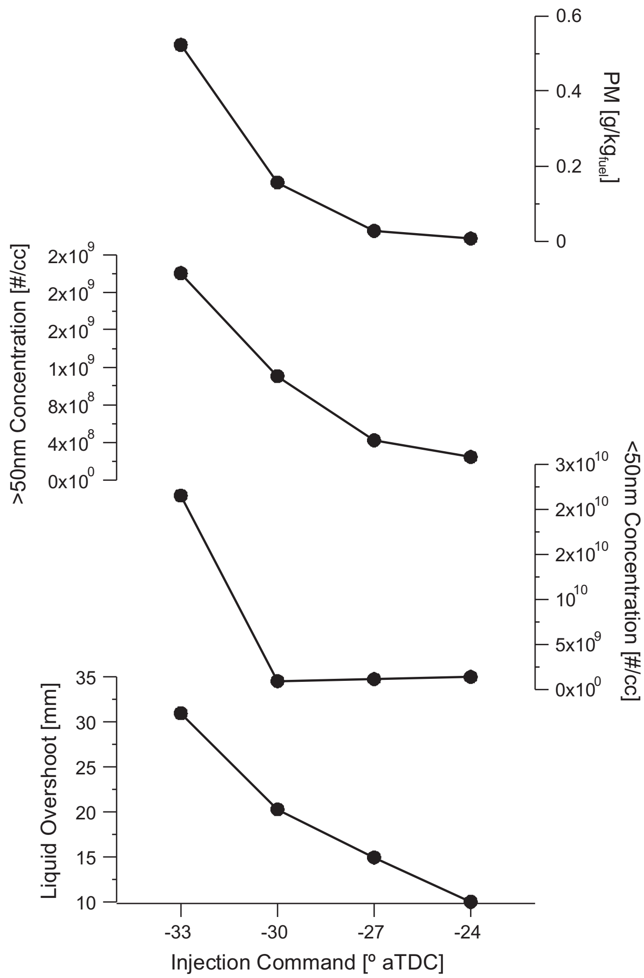

Fig. 7. Comparison of liquid spray overshoot to particle mass and number concentrations.

the flame (thus preventing reduction of the local richness in the high temperature regions of the flame). The diffusion flame on the piston bowl surface would also suffer from a great lack of turbulent mixing energy which is provided in the case of a conventional Diesel diffusion flame from the injected fuel's spray momentum.

The formation pathway of the particles smaller than 50 nm is more difficult to understand than of those larger than 50 nm. Based on [12,13], the nucleation mode particles (typically smaller than 50 nm) are largely composed of volatile material and can contain greater than 90% of the particle numbers. Looking at the increased HC emissions in Fig. 3, it is suggested that there was an increase in engine-out condensable HC material which can contribute to the strong increase in particle emissions smaller than 50 nm in the −33°aTDC injection timing. Kashdan et al. discussed the possibility of liquid fuel deposited on the piston bowl surface to flash boil during the expansion and exhaust strokes when the exhaust valve is opened [46]. But the very large increase in particle numbers smaller than 50 nm from −30 to −33°aTDC did not proportionally correlate to an equally larger increase in the liquid overshoot or overall HC emissions relative to the changes between the other injection timings. Therefore it is suggested that there were other factors not examined in this study, or more specific aspects within the ones discussed, which contributed to the very large increase in particles smaller than 50 nm from −30 to −33°aTDC injection timing. But it remains true that the number of particles larger than 50 nm did change similarly to the change in the liquid overshoot for all injection timings.

3.4. Methods of liquid length reduction

Some possible ways to decrease the HC, CO, and PM emissions by reducing the fuel spray's liquid length and fuel deposits on the piston are discussed in this section. Increasing the engine's intake temperature, and therefore increasing the engine's in-cylinder unburned gas temperatures as well, would increase fuel vaporization and therefore reduce the injected fuel spray's liquid length. But higher intake temperature would also cause the injected fuel to auto-ignite earlier and decrease the ignition delay. As seen in Figs. 2 and 3, decreased ignition delay would decrease the time for fuel and air premixing before combustion, thus increasing PM formation.

Another possible way to decrease the fuel spray's liquid length would be by increasing the in-cylinder charge air density, achievable by increasing the engine's intake pressure. But in order to maintain the same engine intake oxygen concentration or global combustion air/fuel ratio, an increase in EGR rate would be necessary. Since premixed LTC is currently limited to low to mid engine loads, it is already difficult to provide the exhaust turbine of the engine's turbocharger with enough exhaust gas energy to power the intake air compressor to generate moderate levels of intake air boost at these low loads. Depending on the engine, this option may not be possible simply due to turbocharger restrictions.

A final suggestion to decrease the fuel spray's liquid length would be by decreasing the injector nozzle's orifice diameter to increase air entrainment into the spray. While many orifices of small diameters would be interesting for completely premixed LTC (typically only applicable at low engine load conditions) since the injection finishes before the start of combustion, this injector nozzle design could be less advantageous for conventional diffusive mixing-controlled Diesel combustion (which has been proven to function throughout all engine loads and speeds) due to possible jet to jet interactions.

4. Conclusions

Particulate matter mass and number emissions were shown to increase with further advances in the fuel injection timing earlier than −24°aTDC (the early injection timing with <0.05 FSN) within the Diesel LTC regime, contrary to increased ignition delay and $T_{ad}85$. These increases in PM emissions were also contrary to expected PM emissions decreases, based on the reductions in maximum local fuel-equivalence ratio predicted with advanced injection times by the free fuel jet spray model. Using a 1D free spray model, it was shown that increased PM mass, particle number, HC, and CO emissions with advanced fuel injection timings corresponded with higher relative levels of predicted liquid fuel deposition on the piston bowl surface. Therefore it is believed that the increased number of particles larger than 50 nm (and even higher increase in particles smaller than 50 nm) with further advances in injection timing past −24°aTDC in this LTC operating condition were due to increased amounts of fuel deposited on the piston during the injection process. This is especially attested by the increases in predicted fuel liquid spray overshoot and the increase in the particles larger than 50 nm typically formed in the locally rich, high temperature regions of a diffusive Diesel mixing-controlled flame. Ways to reduce particulate emissions from liquid fuel deposition on the piston bowl surface included: increased engine intake temperatures to enhance fuel spray vaporization, increased intake pressure to reduce fuel spray liquid length without greatly reducing ignition delay, or by improved air entrainment into each fuel jet by smaller injector nozzle orifice diameters.

Acknowledgments

The authors sincerely thank Gabriel Alcantarilla, Rogério Jorge Amorim, Simon Arthozoul, and Sara Goska for their great assistance in experimental data collection and post-analysis. The authors wish to acknowledge the Generalitat Valenciana for the financial support through the project GVA PROMETEO CMT 2010 (reference code: GR001/2009/00167539). Financial support of Christopher Kolodziej's research was provided by the Spanish Ministry of Education. This publication comes from a portion of the doctoral thesis work of Christopher Kolodziej.

References

[1] Atkinson RW, Fuller GW, Anderson HR, Harrison RM, Armstrong B. Urban ambient particle metrics and health: a time-series analysis. Epidemiology 2010;21(4):501–11.
[2] Pope III CA, Dockery DW. Health effects of fine particulate air pollution: lines that connect. J Air Waste Manage Assoc 2006;56:709–42.
[3] WHO. Air quality guidelines, global update 2005. Copenhagen: WHO Regional Office for Europe; 2006.
[4] Reichhardt T. Weighing the health risks of airborne particulates. Environ Sci Technol 1995;29(8):360A–4A.
[5] Pekkanen J, Kulmala M. Exposure assessment of ultrafine particles in epidemiologic time-series studies. Scand J Work Environ Health 2004;30(2):9–18.
[6] Donaldson K, Stone V, Seaton A, MacNee W. Ambient particle inhalation and the cardiovascular system: potential mechanisms. Environ Health Perspect 2001;109(4):523–7.
[7] Oberdorster G, Oberdorster E, Oberdorster J. Nanotoxicology: an emerging discipline evolving from studies of ultrafine particles. Environ Health Perspect 2005;113:823–39.
[8] Seaton A, MacNee W, Donaldson K, Godden D. Particulate air pollution and acute health effects. Lancet 1995;345:176–8.
[9] Delfino RJ, Sioutas C, Malik S. Potential role of ultrafine particles in associations between airborne particle mass and cardiovascular health. Environ Health Perspect 2005;113:934–46.
[10] Ibald-Mulli A, Wichmann HE, Kreyling W, Peters A. Epidemiological evidence on health effects of ultrafine particles. J Aerosol Med 2002;15:189–201.
[11] Wichmann HE, Spix C, Tuch T, Wolke G, Peters A, Heinrich J, et al. Epidemiological evidence of the effects of ultrafine particle exposure. Res Rep Health Eff Inst 2000;86(5):87–94.
[12] Kittelson DB. Engines and nanoparticles: a review. J Aerosol Sci 1998;29:575–88.
[13] Montajir RM, Kawai T, Goto Y, Odaka M. Thermal conditioning of exhaust gas: potential for stabilizing diesel nano-particles. SAE 2005-01-0187; 2005.
[14] Kamimoto T, Bae MH. High combustion temperature for the reduction of particulate in diesel engines. SAE 880423; 1988.
[15] Dec JE. A conceptual model of DI diesel combustion based on laser-sheet imaging. SAE 970873; 1997.
[16] Akihama K, Takatori Y, Inagaki K, Sasaki S, Dean AM. Mechanism of the smokeless rich diesel combustion by reducing temperature. SAE 2001-01-0655; 2001.
[17] Kimura S, Aoki O, Kitahara Y, Aiyoshizawa E. Ultra-clean combustion technology combining a low-temperature and premixed combustion concept for meeting future emission standards. SAE 2001-01-0200; 2001.
[18] Okude K, Mori K, Shiino S, Moriya T. Premixed compression ignition (PCI) combustion for simultaneous reduction of NOx and soot in diesel engine. SAE 2004-01-1907; 2004.
[19] Noehre C, Andersson M, Johansson B, Hultqvist A. Characterization of partially premixed combustion. SAE 2006-01-3412; 2006.
[20] Colban WF, Miles PC, Oh S. Effect of intake pressure on performance and emissions in an automotive diesel engine operating in low temperature combustion regimes. SAE 2007-01-4063; 2007.
[21] Raatz T, Mueller E. Examination of particle size distribution of homogeneous and conventional diesel combustion. SAE 2001-01-3576; 2001.
[22] Sluder CS, Wagner RM, Storey JME, Lewis S. Implications of particulate and precursor compounds formed during high-efficiency clean combustion in a diesel engine. SAE 2005-01-3844; 2005.
[23] Ogawa H, Miyamoto N, Shimizu H, Kido S. Characteristics of diesel combustion in low oxygen mixtures with ultra-high EGR. SAE 2006-01-1147; 2006.
[24] Kolodziej C, Wirojsakunchai E, Foster DE, Schmidt N, Kamimoto T, Kawai T et al. Comprehensive characterization of particulate emissions from advanced diesel combustion. SAE 2007-01-1945; 2007.
[25] Natti KC, Henein NA, Poonawala Y, Bryzik W. Particulate matter characterization studies in an HSDI diesel engine under conventional and LTC regime. SAE Int J Engines 2008;1(1):735–45.
[26] Storey JME, Lewis SASr, Parks JEII, Szybist JP, Barone TL, Prikhodko VY. Mobile source air toxics (MSATs) from high efficiency clean combustion: catalytic exhaust treatment effects. SAE Int J Engines 2008;1(1):1157–66.
[27] Opat R, Ra Y, Gonzalez DMA, Krieger R, Reitz RD, Foster DE et al. Investigation of mixing and temperature effects on HC/CO emissions for highly dilute low temperature combustion in a light duty diesel engine. SAE 2007-01-0193; 2007.
[28] Benajes J, Novella R, Arthozoul S, Kolodziej C. Particle size distribution measurements from early to late injection timing low temperature combustion in a heavy duty diesel engine. SAE 2010-01-1121; 2010.
[29] Benajes J, Novella R, Arthozoul S, Kolodziej C. Injection timing effects on premixed LTC particle emissions from light and heavy duty diesel engines. Poster and extended abstract, 14th ETH-Zurich conference on combustion generated nanoparticles; August 2010.
[30] Pastor JV, López JJ, García JM, Pastor JM. A 1D model for the description of mixing-controlled inert diesel sprays. Fuel 2008;87:2871–85.
[31] Desantes JM, Pastor JV, García-Oliver JM, Pastor JM. A 1D model for the description of mixing-controlled reacting diesel sprays. Combust Flame 2009;156:234–49.
[32] Baumgard KJ, Johnson JH. The effect of fuel and engine design on diesel exhaust particle size distributions. SAE 960131; 1996.
[33] Bielaczyc P, Merkisz J, Kozak M. Analysis of the influence of fuel sulfur content on diesel engine particulate emissions. SAE 2002-01-2219; 2002.
[34] Mitchell K, Steere DE, Taylor JA, Manicom B, Fisher JE, Sienicki EJ et al. Impact of diesel fuel aromatics on particulate, PAH and nitro-PAH emissions. SAE 942053; 1994.
[35] Liu ZG, Vasys VN, Kittelson DB. Nuclei-mode particulate emissions and their response to fuel sulfur content and primary dilution during transient operations of old and modern diesel engines. Environ Sci Technol 2007;41:6479–83.
[36] Den Ouden CJJ, Clark RH, Cowley LT, Stradling RJ, Lange WW, Maillard C. Fuel quality effects on particulate matter emissions from light- and heavy-duty diesel engines. SAE 942022; 1994.
[37] TSI Incorporated. Aerosol instrument manager software for scanning mobility particle sizer (SMPS) spectrometer. Rev. G. P/N 1930038; October 2006.
[38] Bosch W. Fuel rate indicator is a new instrument for display of the characteristics of individual injection. SAE 660749; 1966.
[39] Way RJB. Methods for determination of composition and thermodynamic properties of combustion products for internal combustion engine calculations. Proc IME 1976;190:686–97.
[40] Lapuerta M, Armas O, Hernández JJ. Diagnostic of D.I. diesel combustion from in-cylinder pressure signal by estimation of mean thermodynamic properties of the gas. Appl Therm Eng 1999;19:513–29.
[41] Payri F, Molina S, Martín J, Armas O. Influence of measurement errors and estimated parameters on combustion diagnosis. Appl Therm Eng 2006;26:226–36.
[42] Fang T, Coverdill RE, Lee CF, White RA. Smokeless combustion within a small-bore HSDI diesel engine using a narrow angle injector. SAE 2007-01-0203; 2007.
[43] Martin GC, Mueller CJ, Milam DM, Radovanovic MS, Gehrke CR. Early direct-injection, low-temperature combustion of diesel fuel in an optical engine utilizing a 15-hole, dual-row, narrow-included-angle nozzle. SAE 2008-01-2400; 2008.
[44] Kook S, Pickett LM, Musculus MPB. Influence of diesel injection parameters on end-of-injection liquid length recession. SAE 2009-01-1356; 2009.
[45] Pickett LM, Kook S, Williams TC. Transient liquid penetration of early-injection diesel sprays. SAE 2009-01-0839; 2009.
[46] Kashdan JT, Mendez S, Bruneaux G. On the origin of unburned hydrocarbon emissions in a wall-guided, low NOx diesel combustion system. SAE 2007-01-1836; 2007.